MO parameters. Shortcomings of MO problems for conformational analysis and for calculating heats of formation are not carried over here.

This type of simulation scheme is particularly valuable for large molecules since it is a fast and general method assuming that all the force constants are known. The method presented here has been extensively tested by examining a large, diverse group of conjugated hydrocarbons. Many systems which cannot be treated well by previous methods are handled satisfactorily by this method. The accuracy of the results is competitive with that of high-quality experimental work. The extension of this approach to conjugated systems containing heteroatoms will be described elsewhere.

Acknowledgment. Thanks to our management, R. Thomson and R. Waugh, for their support and Dr. A. Lilly and Dr. J. Seeman for their comments.

Methyl Group Dynamics from Relaxation of Double Quantum Filtered NMR Signals: Application to Deoxycholate

Lewis E. Kay[†] and J. H. Prestegard*[‡]

Contribution from the Departments of Molecular Biophysics and Biochemistry and Chemistry, Yale University, New Haven, Connecticut 06511. *Received October 15, 1986*

Abstract: An experimental procedure and a theoretical analysis are developed for the extraction of cross-correlation spectral densities from proton NMR resonances of A_3 spin systems. The experiment involves observation of forbidden peak intensities of double quantum filtered one-dimensional spectra as a function of excitation time. When used in combination with T_1 and T_2 data sets, this experiment provides the additional information necessary to characterize multiple internal motions exhibited by groups which contain A_3 spin systems. These methods are applied to isolated methyl groups in micelles of deoxycholate (DOC). Results obtained from simultaneous fits of T_1, T_2, and forbidden peak intensities indicate that the methyls attached to the steroid nulceus are highly ordered, with internal rotations consistent with current micelle models. Prospects for qualitative characterization of internal motions from 2-D spectra are also assessed.

The potential for obtaining information on the structure and dynamics of macromolecular assemblies has advanced substantially over the past few years through the introduction of two-dimensional NMR methods. These methods have made it possible to extract cross-relaxation times from very complex proton NMR spectra. These cross-relaxation times, when converted to interproton distance constraints, form the basis for recent efforts in structure determination.[1,2] These experiments and the interpretation of resulting data are complicated, however, by the fact that protons on many of the more easily observed groups (for example, methyl groups) have interactions modulated by internal as well as overall molecular motion. In assemblies involving many molecules (for example, membrane systems), interactions among spins may also be modulated by both inter- and intramolecular motions. These complicating effects make it difficult to convert observed cross-relaxation times to useful distance information or motional parameters. The idea that some of these complicating factors could be separated on the basis of data available in existing or slightly modified 2-D NMR experiments is an appealing one and is a principal motivation for this study.

Recently, Muller et al. reported on the appearance of forbidden cross-peaks in ^1H multiple quantum filtered correlation spectroscopy and multiple quantum NMR.[3] Typically n quantum filtered spectra consist of peaks associated with spins having resolved scalar couplings to at least $(n - 1)$ equivalent or nonequivalent spins.[4] A simple example where "forbidden" peaks arise in such spectra is in the case of a methyl group connected to a tertiary carbon. In this case, the methyl group forms an A_3 spin system. On the basis of a simple theoretical formalism for multipulse experiments, the single resonance associated with this system should be removed by a multiple quantum filter. Multiple quantum peaks associated with degenerate spin systems of this type do, however, appear in spectra of macromolecules.[3,5,6] While these cross-peaks may complicate interpretation of two-dimensional (2-D) NMR data sets for the purpose of spectral assignment, we believe that their appearance can provide useful information on the motional properties of the participating spins, and ultimately structural properties of the parent molecule. This is due to the fact that the appearance of such forbidden peaks is a direct consequence of cross-correlation effects between pairs of spins.

Previous studies, pioneered by the Volds and co-workers[7,8] and Grant and co-workers[9] have shown cross-correlation spectral density terms to be extremely useful in the extraction of dynamic properties of spin systems. Most spin systems considered to date have been heteronuclear AX_2 or AX_3 systems involving either ^{13}C[7,8] or ^{19}F[10] and ^1H. However, homonuclear cases are quite analogous. Methods of extracting cross-correlation spectral density terms from ^{13}C or ^{19}F spectra have been based largely on fitting T_1 and T_2 relaxation data. Recently, however, Bendall and coworkers have identified cross-correlation effects in methyl groups using polarization transfer sequences such as DEPT and INEPT,[11] while Brondeau and co-workers have developed elegant heteronuclear multipulse schemes to determine cross-correlation spectral density terms for $^{13}CH_2$ groups.[12] A potential drawback of these methods is that they require isotopic enrichment which may prove

[†] Department of Molecular Biophysics and Biochemistry.
[‡] Department of Chemistry.

(1) Holak, T. A.; Prestegard, J. H. *Biochemistry* **1986**, *25*, 5766.
(2) Williamson, H. P.; Havel, T. F.; Wuthrich, K. *J. Mol. Biol.* **1985**, *182*, 295.
(3) Muller, N.; Bodenhausen, G.; Wuthrich, K.; Ernst, R. R. *J. Magn. Reson.* **1985**, *65*, 531.
(4) Piantini, U.; Sorensen, O. W.; Ernst, R. R. *J. Am. Chem. Soc.* **1982**, *104*, 6801.
(5) Rance, M.; Wright, P. E. *Chem. Phys. Lett.* **1986**, *124*, 572.
(6) Muller, N.; Ernst, R. R.; Wuthrich, K. *J. Am. Chem. Soc.* **1986**, *108*, 6482.
(7) Vold, R. L.; Vold, R. R. Prog. *NMR Spectrosc.* **1978**, *12*, 79.
(8) Vold, R. R.; Vold, R. L. *J. Chem. Phys.* **1976**, *64*, 320.
(9) Werbelow, L. G.; Grant, D. M. *Adv. Magn. Reson.* **1977**, *9*, 189.
(10) Prestegard, J. H.; Grant, D. M. *J. Am. Chem. Soc.* **1978**, *100*, 4664.
(11) Bendall, M. R.; Pegg, D. T. *J. Magn. Reson.* **1983**, *53*, 40.
(12) Brondeau, J.; Canet, D.; Millot, C.; Nevy, H.; Werbelow, L. *J. Chem. Phys.* **1985**, *82*, 2212.

0002-7863/87/1509-3829$01.50/0

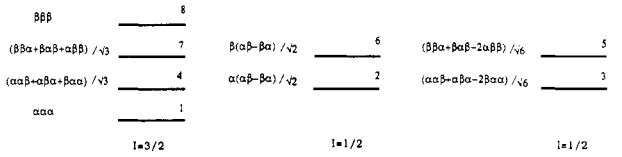

Figure 1. Energy level diagram and wave functions for an A_3 spin system written in an irreducible basis representation.

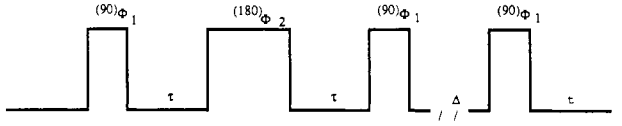

Figure 2. Pulse sequence used to generate double quantum filtered spectra.

difficult or impossible for many biomolecules. In the case of T_1 and T_2 relaxation data, cross-correlation terms manifest themselves largely as small deviations from nearly exponential decays, and accurate extraction of cross-correlation spectral density terms requires very precise measurements. Also, intragroup dipolar cross-correlation effects measured in T_1 and T_2 studies, especially in methyl groups, may be masked by other interactions such as spin rotation and dipolar interactions with neighboring protons.[13,14] While for certain cases it has been possible to extract nonexponential relaxation times from T_1 profiles,[14,15] we feel that in general cross-correlation terms may be more readily extracted from the appearance of forbidden peaks in multiple quantum filtered one- and two-dimensional spectra.

In principal, measurement of forbidden peak intensity as a function of delays between multiple quantum excitation pulses should provide a sensitive probe of cross-correlation spectral density terms. This is due to the fact that in the absence of such terms degenerate transitions of spin systems of the type A_nX_m will decay uniformly. In this case complete cancellation of magnetization from different coherence transfer processes will occur so that degenerate X magnetization cannot be transferred into X multiple quantum coherence.[16] In an exactly analogous fashion X multiple quantum coherence cannot be transferred into one quantum X magnetization for observation. The effect of correlated motions is to give rise to nonuniform decays of magnetization associated with degenerate transverse elements so that incomplete cancellation of different coherence transfer processes occurs and excitation of multiple quantum coherence becomes allowed.[3]

In this paper we wish to report an investigation of the motional properties of an X_3 spin system using forbidden peak intensities from a one-dimensional analogue of the double quantum 2-D experiment in which such peaks have been previously observed. The molecule chosen for this study is the bile salt, sodium deoxycholate (DOC), which forms micelles of molecular weight comparable to many medium-sized proteins. The molecule contains several isolated X_3 (CH_3) systems and hence is a suitable test system for the experiments proposed. The appearance of CH_3 peaks in a one-dimensional double quantum filtered spectrum when combined with T_1 and T_2 data should provide information concerning both methyl group and micelle dynamics. The properties of these micelles are of substantial interest in their own right, and in addition to demonstrating the use of forbidden multiple quantum peaks in extracting dynamic information, we hope to contribute to an understanding of the DOC system.

Theory

Figure 1 shows an energy level diagram and associated wave functions for an X_3 spin system. The effects of the double quantum filtered pulse sequence, shown in Figure 2, including relaxation can be understood by considering the equations describing density matrix evolution.[17] Noting that the $I = {}^3/_2$ manifold is not mixed with either $I = {}^1/_2$ manifolds upon application of rf pulses and noting also that it is only possible to generate multiple quantum coherence (MQC) in the $I = {}^3/_2$ manifold leads initially to a consideration of a simplified density matrix, $\rho^{I=3/2}$, which is 4×4 rather than 8×8. We have, at equilibrium,

$$\rho^{I=3/2} = {}^1/_4\mathbf{1} + (\omega_0\hbar/8kT)\begin{bmatrix} 3 & 0 & 0 & 0 \\ 0 & 1 & 0 & 0 \\ 0 & 0 & -1 & 0 \\ 0 & 0 & 0 & -3 \end{bmatrix} \quad (1)$$

where ω_0 is the resonance frequency of the X_3 spin system, k is Boltzmann's constant, and $\mathbf{1}$ denotes the unit matrix. Since $\mathbf{1}$ is invariant to the action of pulses, we neglect it in the future and concern ourselves only with the second term in eq 1. Phases of pulses in the pulse sequence of Figure 2 are cycled so that magnetization acquired during t is modulated only by double quantum coherence during the period Δ. Initially we consider only the line of the phase cycling scheme in which phases of all pulses are $\pi/2$ (see Table I). Application of a 90_y pulses gives

$$\rho^{I=3/2} \propto \begin{bmatrix} 0 & \sqrt{3} & 0 & 0 \\ \sqrt{3} & 0 & 2 & 0 \\ 0 & 2 & 0 & \sqrt{3} \\ 0 & 0 & \sqrt{3} & 0 \end{bmatrix} \quad (2)$$

The effect of the 180_y pulse applied at τ is to refocus chemical shift offset so that at 2τ magnetization dispersed through chemical shift is refocused. Since we are working with a spin system in which no scalar coupling is resolved, the only effects remaining at the end of 2τ are those associated with transverse relaxation. For ^{1}H NMR solution studies it is often sufficient to consider relaxation effects originating from ^{1}H dipolar interactions only.[13] We will write the relaxation Hamiltonian as

$$\mathcal{H}(t) = \sum_{i<j}\epsilon_{ij}\sum_m(-1)^m T_2^m(i,j)Y_2^{-m}(\phi_{ij}) + \sum_i\gamma_i\sum_m(-1)^m T_1^m(i)B_1^{-m}(i,t) \quad (3)$$

where the first term considers explicitly the contributions to relaxation due to pairwise dipolar interactions among any of the three methyl spins and the second term is used to approximate remaining interactions. The equations would be rigorous if the only additional interactions were dipolar interactions with nonresonating nuclei and spin rotation interactions.[7,9] However, it is cleary an approximation in cases where intramolecular interactions of the A_3 spin system with other geometrically constrained nuclei exist. Given the data available in experiments to be discussed here, a more complete theoretical description is not possible at this time. In eq 3, $\epsilon_{ij} = \sqrt{6}\pi/5\gamma_i\gamma_j\hbar/r_{ij}^3$, $T_2^m(i,j)$ is a dipolar spin tensor operator of rank 2 connecting spins i and j, $Y_2^{-m}(\phi_{ij})$ is a spherical harmonic of rank 2 whose value depends on the orientation of the i–j dipolar vector relative to the external field, T_1^m is a first rank spin tensor, and $B_1^{-m}(i,t)$ is a lattice random field interaction operator. We assume that the random fields are isotropic, i.e., $|B_1^0(i,t)|^2 = |B_1^{+1}(i,t)|^2 = |B_1^{-1}(i,t)|^2$.[9]

Table I. Phase Cycling Employed in the Selection of Double Quantum Filtered Spectra

$\phi_1{}^a$	$\phi_2{}^b$	receiver phase	$\phi_1{}^a$	$\phi_2{}^b$	receiver phase
x	x	x	x	$-x$	$-x$
y	x	$-x$	y	$-x$	x
$-x$	x	x	$-x$	$-x$	$-x$
$-y$	x	$-x$	$-y$	$-x$	x
x	y	$-y$	x	$-y$	y
y	y	y	y	$-y$	$-y$
$-x$	y	$-y$	$-x$	$-y$	y
$-y$	y	y	$-y$	$-y$	$-y$

[a] Phase of excitation pulses. [b] Phase of observation pulses.

(13) Werbelow, L. G.; Marshall, A. G. *J. Magn. Reson.* **1973**, *11*, 299.
(14) Rodrigues De Miranda, J. F.; Hilbers, C. W. *J. Magn. Reson.* **1975**, *19*, 11.
(15) Haslinger, E.; Kalchhauser, H.; Robien, W. *J. Mol. Liq.* **1984**, *28*, 223.
(16) Braunschweiler, L.; Bodenhausen, G.; Ernst, R. R. *Mol. Phys.* **1983**, *48*, 533.
(17) Slichter, C. P. *Principles of Magnetic Resonance*, 2nd ed.; Springer: Berlin, 1978.
(18) Redfield, A. G. *Adv. Magn. Reson.* **1965**, *1*, 1.

Table II. Redfield Elements for Transverse Relaxation

element	$J_A(0)^a$	$J_C(0)^b$	$J_A(\omega)$	$J_C(\omega)$	$J_A(2\omega)$	$J_C(2\omega)$	$j(0)^c$	$j(\omega)^c$	$j(0)^d$	$j(\omega)^d$
1414	−3	−3	4	2	−4	−2	−1	5	−1	3
1426	0	0	$\sqrt{3}/2$	$-\sqrt{3}/2$	0	0	0	0	0	$-1/\sqrt{3}$
1435	0	0	$-\sqrt{3}/2$	$\sqrt{3}/2$	0	0	0	0	0	$1/\sqrt{3}$
1447	0	0	0	0	0	0	0	$-2\sqrt{3}$	0	$-2/\sqrt{3}$
1478	0	0	0	0	2	4	0	0	0	0
2626	−1	1	2	−2	−2	2	−1	1	−2	3
2635	0	0	0	0	0	0	0	0	1/3	0
2647	−1	1	0	0	0	0	0	0	2/3	0
2678	0	0	$\sqrt{3}/2$	$-\sqrt{3}/2$	0	0	0	0	0	$-1/\sqrt{3}$
3535	−1	1	2	−2	−2	2	−1	1	−2	3
3547	1	−1	0	0	0	0	0	0	−2/3	0
3578	0	0	$-\sqrt{3}/2$	$\sqrt{3}/2$	0	0	0	0	0	$1/\sqrt{3}$
4747	−2	2	5	1	−2	−4	−1	7	−5/3	3
4778	0	0	0	0	0	0	0	$-2\sqrt{3}$	0	$-2/\sqrt{3}$
7878	−3	−3	4	2	−4	−2	−1	5	−1	3

[a] $J_A(0)$ is the auto-spectral density function evaluated at $\omega = 0$. [b] $J_C(0)$ is the cross-sectional density function evaluated at $\omega = 0$. [c] Terms obtained by setting random auto- and cross-spectral density functions equal. [d] Terms obtained by setting random cross-spectral densities to zero.

In general, dipolar relaxation couples transverse elements of coherence from the $I = {}^3/_2$ manifold with elements from the $I = {}^1/_2$ manifolds so that for relaxation effects we must consider elements from the full density matrix. Using Redfield theory[13] to describe relaxation during the excitation and acquisition periods we have

$$d\vec{\rho}/dt = \mathbf{R}\vec{\rho} \tag{4}$$

with $\vec{\rho} = (\rho_{14},\rho_{26},\rho_{35},\rho_{47},\rho_{78})$ and $\mathbf{R}$ a Redfield relaxation matrix whose dipolar part is given by:[9]

$$R^{ijkl}_{\alpha\sigma\nu\epsilon} = \sum_{m,n}\{2J^{mn}_{ijkl}(\omega_{\alpha\nu})\langle\alpha|T^m_2(i,j)|\nu\rangle\langle\epsilon|T^n_2(k,l)|\sigma\rangle - \delta_{\alpha\nu}\sum_\beta J^{mn}_{ijkl}(\omega_{\epsilon\beta})\langle\epsilon|T^m_2(i,j)|\beta\rangle\langle\beta|T^n_2(k,l)|\sigma\rangle - \delta_{\sigma\epsilon}\sum_\beta J^{mn}_{ijkl}(\omega_{\nu\beta})\langle\alpha|T^m_2(i,j)|\beta\rangle\langle\beta|T^n_2(k,l)|\nu\rangle\} \tag{5}$$

In eq 5 $J^{mn}_{ijkl}(\omega)$ is a spectral density function given by

$$J^{mn}_{ijkl}(\omega) = \epsilon_{ij}\epsilon_{kl}\int_0^\infty \langle Y^m_2(\phi_{ij}(t))Y^n_2(\phi_{kl}(t+\tau))\rangle \cos\omega\tau\, d\tau \tag{6}$$

Spectral densities are referred to as auto-correlation spectral densities when the orientation of a dipole vector at time t is related to the orientation of the same vector at time $t + \tau$ (i.e., $ij = kl$). In contrast, cross-correlation spectral densities relate the orientation of the ij dipolar vector at time t to the kl vector at time $t + \tau$ for $ij \neq kl$. Many treatments of spin relaxation assume $J_{ijkl}(\omega) = 0$ when $ij \neq kl$. We explicitly avoid this assumption in what follows. Completely analogous expressions can be written for the random field part of $\mathbf{R}$ in terms of random-field spectral densities. Table II contains a complete listing of the elements of $\mathbf{R}$ in terms of auto- and cross-spectral densities.

Spectral densities can be evaluated more explicitly by considering an appropriate motional model for describing the dynamics of methyl groups within a spherical DOC micelle.[19] We have modified the cone model of Brainard and Szabo[20] using the method of Hubbard[21] to yield expressions for the appropriate auto- and cross-spectral density functions. They are

$$J^{mn}_{ijkl}(\omega) = {}^3/_{10}(-1)^n\gamma^4\hbar^2/r^6\delta_{m-n}[{}^1/_4S^2 6D/[(6D)^2+\omega^2] + {}^1/_4(1-S^2)(6D + 6D_w/(1-S^2))/[(6D + 6D_w/(1-S^2))^2+\omega^2] + {}^3/_4\cos(\Omega_{ijkl})S^2(6D+4D_\parallel)/[(6D+4D_\parallel)^2+\omega^2] + {}^3/_4\cos(\Omega_{ijkl})(1-S^2)(6D+4D_\parallel+2D_w/(1-S^2))/[(6D+4D_\parallel+2D_w/(1-S^2))^2+\omega^2]] \tag{7}$$

The model is depicted in Figure 3 with the relationship of parameters to molecular motion indicated. In the model we have assumed that the DOC micelle is spherical[19] and has a rotational correlation time of ${}^1/_6D$, and that the C_∞ axis of the methyl group rotates with a correlation time of ${}^1/_4D_\parallel$. The C_∞ axis in turn

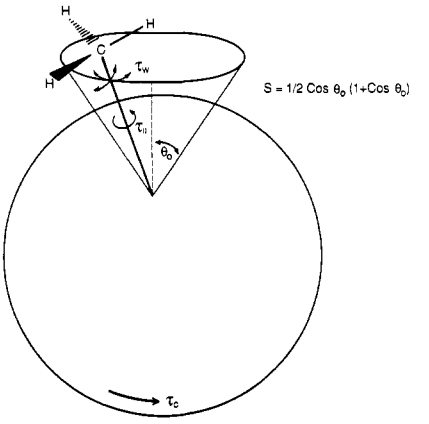

Figure 3. Cone model of Brainard and Szabo[20] describing the motion of a methyl group in a spherical micelle. τ_c is the isotropic rotational correlation time of the micelle, $\tau_\parallel$ is the internal methyl rotational correlation time, and τ_w is the correlation time describing the wobbling of the C_∞ axis of the methyl group in a cone of angle θ_0.

"wobbles" within a cone of angle θ with a frequency of $6D_w$ and an order parameter of S. S can be related to θ by

$$S_{cone} = {}^1/_2\cos\theta\,(1+\cos\theta) \tag{8}$$

which assumes that there is a constant potential function describing diffusion in the cone.[20] Finally Ω_{ijkl} is the angle that the i–j ^{1}H–^{1}H vector makes with the k–l ^{1}H–^{1}H vector. For the case of autospectral density terms, $ij = kl$ and therefore $\Omega_{ijkl} = 0$, while in the case of three protons oriented at the vertices of an equilateral triangle (CH_3 group) with $ij \neq kl$, $\Omega_{ijkl} = 60°$. Equation 4 can be solved using standard matrix techniques[9] to give:

$$\vec{\rho}(t) = \mathbf{Q}\exp(-\mathbf{Q}^{-1}\mathbf{R}\mathbf{Q}t)\mathbf{Q}^{-1}\vec{\rho}(0) \tag{9}$$

where $\mathbf{Q}$ is a matrix of eigenvectors of $\mathbf{R}$, $\mathbf{Q}^{-1}$ is the inverse of matrix $\mathbf{Q}$, and $\vec{\rho}(0)$ contains the values of the transverse elements of the density matrix at the outset of the relaxation period.

Immediately before application of the second 90_y pulse $\rho^{I=3/2}$ can be written

$$\rho^{I=3/2} = \begin{bmatrix} 0 & \rho_{14}(2\tau) & 0 & 0 \\ \rho^*_{14}(2\tau) & 0 & \rho_{47}(2\tau) & 0 \\ 0 & \rho^*_{47}(2\tau) & 0 & \rho_{78}(2\tau) \\ 0 & 0 & \rho^*_{78}(2\tau) & 0 \end{bmatrix} \tag{10}$$

Application of the second 90_y pulse gives rise to double quantum coherence ρ_{17}, ρ_{48} with

$$\rho_{17}(2\tau^+) \propto \rho_{14}(2\tau^-) + \sqrt{3}\rho_{47}(2\tau^-) - 3\rho_{78}(2\tau^-) - 3\rho^*_{14}(2\tau^-) + \sqrt{3}\rho^*_{47}(2\tau^-) + \rho^*_{78}(2\tau^-)$$

$$\rho_{48}(2\tau^+) \propto 3\rho_{14}(2\tau^-) - \sqrt{3}\rho_{47}(2\tau^-) - \rho_{78}(2\tau^-) - \rho^*_{14}(2\tau^-) - \sqrt{3}\rho^*_{47}(2\tau^-) + 3\rho^*_{78}(2\tau^-) \tag{11}$$

(19) Small, D. M. *The Bile Acids*; Plenum Press: New York, 1971; p 249.
(20) Brainard, J. R.; Szabo, A. *Biochemistry* **1981**, *20*, 4618.
(21) Hubbard, J. R. *J. Chem. Phys.* **1970**, *52*, 563.

ρ^*_{ij} is the complex conjugate of ρ_{ij}, and $\rho(2\tau^-)$, $\rho(2\tau^+)$ denote the value of ρ before and after the second pulse, respectively. We note that in the absence of relaxation,

$$(\rho_{14}(2\tau^-),\rho_{47}(2\tau^-),\rho_{78}(2\tau^-)) = (\sqrt{3},2,\sqrt{3})$$

and substitution into eq 11 leads to $\rho_{17} = \rho_{48} = 0$ in agreement with coherence transfer selection rules derived by Ernst and coworkers.[16] It should be recognized, however, that, in general, nonuniform relaxation of the transverse elements ρ_{14}, ρ_{47}, and ρ_{78} will occur leading to the creation of multiple quantum coherence in A_3 spin systems despite the fact that no resolvable J coupling exists.

Linear combinations of the phase cycling scheme depicted in Table I eliminates all but second-order coherence, and hence from here on we will focus only on these terms. The multiple quantum evolution period, Δ, is sufficiently short ($\Delta = 5$ μs) so that no evolution or relaxation occurs during this interval. Application of the final 90_y pulse establishes single quantum coherence and accordingly:

$$\begin{aligned}\rho_{14}(2\tau + \Delta) &= (3\rho^*_{17} + \rho^*_{48} - \rho_{17} - 3\rho_{48})\\ \rho_{47}(2\tau + \Delta) &= (-\sqrt{3}\rho^*_{17} + \sqrt{3}\rho^*_{48} - \sqrt{3}\rho_{17} + \sqrt{3}\rho_{48}) \quad (12)\\ \rho_{78}(2\tau + \Delta) &= (-\rho^*_{17} - 3\rho^*_{48} + 3\rho_{17} + \rho_{48})\end{aligned}$$

with ρ_{17} and ρ_{48} given by eq 11. During the acquisition time, t, evolution due to both chemical shift and relaxation occurs simultaneously. The effects of these processes can be included by substituting ρ given in eq 13

$$\rho = \begin{bmatrix}\rho_{14}(2\tau+\Delta+t)\\ \rho_{47}(2\tau+\Delta+t)\\ \rho_{78}(2\tau+\Delta+t)\end{bmatrix} = \begin{bmatrix}\rho_{14}(2\tau+\Delta)\\ \rho_{47}(2\tau+\Delta)\\ \rho_{78}(2\tau+\Delta)\end{bmatrix} \exp(-i\omega_0 t) \quad (13)$$

for $\rho(0)$ given in eq 9. Finally, the x component of magnetization, M_x, can be evaluated according to

$$M_x = \gamma\hbar\ \mathrm{Tr}(\rho \mathbf{I}_x) = \gamma\hbar(\sqrt{3}\rho_{14} + 2\rho_{47} + \sqrt{3}\rho_{78} + \sqrt{3}\rho^*_{14} + 2\rho^*_{47} + \sqrt{3}\rho^*_{78}) \quad (14)$$

In the absence of relaxation during the acquisiton period t, eq 13 can be inserted directly into eq 14, and eq 12 used to evaluate density matrix elements giving $M_x = 0$. This emphasizes the fact that in order for forbidden peaks arising from A_3 spin systems to be observed in a multiple quantum filtered spectrum, relaxation must occur during both excitation and acquisition periods. Moreover, if forbidden peaks are to arise, ρ_{14} and ρ_{47} must relax differently. The details of relaxation are given by eq 9 but in certain limiting cases, such as when $J(0)$ terms dominate relaxation, it is easy to show that this can only occur when cross-correlation terms are nonzero. This case is considered explicitly in the Appendix.

From the equations for $\rho_{14}(t)$, $\rho_{47}(t)$, and $\rho_{78}(t)$ given in the Appendix, it is also easy to show that in the limit of short multiple quantum excitation times the intensity of forbidden peaks is a function of cross-correlation spectral density terms only. This is to be contrasted with the situation for T_1 and T_2 relaxation data where in the limit of short relaxation periods cross-correlation terms cancel and magnetization is proportional to auto terms only.[22] This suggests that in the limit $\omega\tau_c \gg 1$, where $J(0)$ terms dominate, it should be possible to measure both auto- and cross-spectral density terms from the slopes of T_2 and multiple quantum filtered relaxation profiles extrapolated to zero relaxation or excitation time, respectively. Hence simultaneous fitting of relaxation data obtained from forbidden peak intensities and conventional T_1 and T_2 experiments should enable accurate extraction of both auto- and cross-correlation terms.

The fact that relaxation is crucial for the excitation and detection of multiple quantum coherence in degenerate spin systems has thus been established theoretically for the specific case of an A_3 system. By varying the time between application of the 90° excitation pulses in the sequence depicted in Figure 2, and by monitoring the resulting double quantum filtered A_3 signal, it is possible to obtain a relaxation profile much like a T_1 or T_2 profile which can be fit to the appropriate dynamical model in order to extract motional parameters. In the subsequent sections we illustrate this approach.

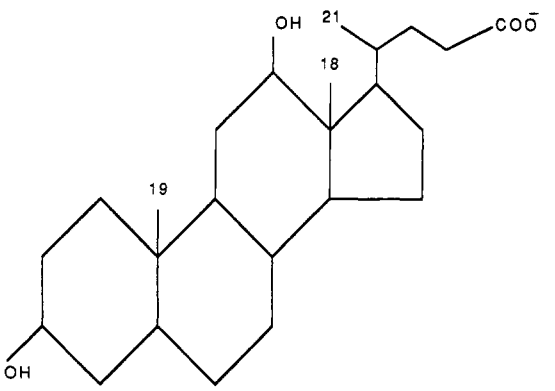

Figure 4. Structure of DOC.

Experimental Section

Sodium deoxycholate was purchased from Calbiochem (La Jolla, CA) and made up to either 15 mM or 50 mM in D_2O, 0.1 M Na_2CO_3, p^2H 9.0. NMR spectra were acquired at 25 °C on a Bruker 500 MHz spectrometer operating in the Fourier transform mode. T_1 relaxation data were obtained using the inversion recovery pulse sequence with a repetition rate of at least $5 \times T_1$. A total of four scans were acquired for each T_1 point. T_2 relaxation data were obtained by using the Carr Purcell Meiboom Gill pulse sequence with either 4- or 8-ms delays between successive 180° pulses.[23] Eight scans per point were obtained and recycling delays of at least $5 \times T_1$ were used. Double quantum filtered spectra were acquired with the pulse sequence and phase cycling scheme described in Figure 2 and Table I, respectively.[24] Typically either 160 or 320 scans were acquired with relaxation delays of $5 \times T_1$. A sweep width of 5000 Hz was employed and 8K data points were collected for all spectra. Double quantum filtered spectra were zero-filled to 16K before transforming. Although double quantum filtered spectra are of high signal to noise ratio, they have phase properties and line shapes that make them difficult to quantitate. To minimize problems, the spectra were displayed in the magnitude corrected mode, $\sqrt{(R(\omega)^2 + I(\omega)^2)}$, where $R(\omega)$ and $I(\omega)$ are data from the real and imaginary channels, respectively and were not apodized for resolution or sensitivity enhancement. For all relaxation experiments considered, peak intensities were obtained by using peak integration software supplied by Bruker.

DOC micelle size distributions were characterized by quasi-elastic light scattering measurements. The samples were prepared in a manner identical with that of the NMR samples except that buffers were filtered through a 1-μm Millipore filter and samples centrifuged at 300 gs for 10 min to remove dust particles. The light scattering measurements were made using an argon ion laser, λ 488 nm, and a Malvern light scattering cell. An autocorrelation function was generated by a Malvern k7025 4-bit correlator and analyzed with an LSI-11 computer. The sample temperature was regulated at 25 °C and the scattering angle used was 90°. The auto-correlation functions were fit according to the cumulant expansion procedure of Koppel[25] and Bargeron[26] using either two or three cumulants. The most probable micelle radius was calculated from the first cumulant using the Stokes–Einstein equation. The second and third cumulants are small, suggesting a homogeneous particle size distribution.

T_1, T_2, and multiple quantum relaxation curves were fit simultaneously using the program STEPIT (copyright 1965, J. P. Chandler, Quantum Chemistry Program Exchange, Indiana University). Guesses for initial values of correlation times and random field terms were input, and from these parameters theoretical multiple quantum curves are calculated using eq 11. Equations analogous to eq 11 were derived for T_1, T_2, and theoretical curves calculated. χ^2 (the sum of the squares of the difference

(22) Kalk, A.; Berendsen, H. J. C. *J. Magn. Reson.* **1976**, *24*, 343.

(23) Car, H. Y., Purcell, E. M. *Phys. Rev.* **1954**, *94*, 630.

(24) Bax, A. *Two-Dimensional Nuclear Magnetic Resonance in Liquids*; Delft University Press: Dordrecht, 1982.

(25) Koppel, D. E. *J. Chem. Phys.* **1972**, *57*, 4814.

(26) Bargeron, C. B. *J. Chem. Phys.* **1974**, *61*, 2134.

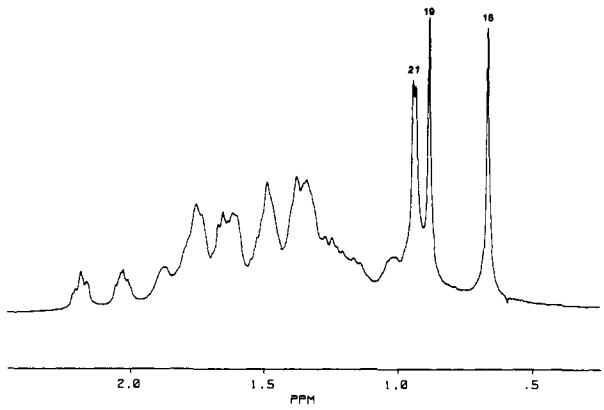

Figure 5. NMR spectrum of DOC micelles at 15 mM, 0.1 M Na_2CO_3, pD 9.0. The spectrum was recorded on a Bruker 500-MHz spectrometer with a sweep width of 5000 Hz; 16 scans of 8K data points were collected and a line broadening of 0.5 Hz was employed.

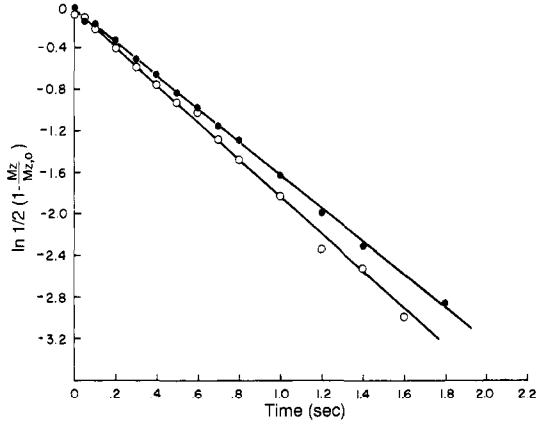

Figure 6. T_1 relaxation curves for DOC samples at concentrations of 15 mM (open circles) and 50 mM (closed circles). A total of four scans were acquired for each T_1 point. Other parameters are the same as for Figure 5.

between experimental and theoretical points) was calculated and minimized by systematically varying the parameters input. Several initial guesses were input to ensure that the parameters obtained from the fit corresponded to a true minimum in χ^2.

Results

Figure 4 shows the chemical structure of DOC, and its associated one-dimensional NMR spectrum is presented in Figure 5. Of the three methyl groups in DOC, the NMR spectrum shows that methyl groups #18 and #19 located at 0.657 and 0.879 ppm, respectively (HDO = 4.72 ppm), can be considered as isolated A_3 spin systems, and methyl group #21 at 0.943 ppm can be considered to be the X_3 part of an AX_3 spin system. We focus our attention on methyl #18 since its resonance is very well-resolved. Figure 6 shows T_1 relaxation data from methyl #18 for samples prepared to 15 and 50 mM in DOC. Data are presented as ln (intensity) vs. time plots so that in the absence of correlated motions a straight line would result. Figure 7 presents transverse relaxation data from these DOC samples. These relaxation curves, in combination with viscosity measurements of DOC solutions which showed no change in viscosity over the concentration range used, suggest that the number of DOC monomers per micelle increases slightly as a function of monomer concentration. While this is hardly a surprising result, a search of the literature reveals that most studies of the physical chemical properties of bile salts have been done at different bile salt concentrations and at variable pH or buffer ionic strength.[19] This makes comparison of our results directly with the literature difficult. Examination of the shape of the T_1 and T_2 relaxation curves reveals that the T_1 curve is nearly linear while the T_2 curve displays a slight nonlinearity. This suggests a complex relaxation behavior, most likely resulting from cross-correlation effects. Given

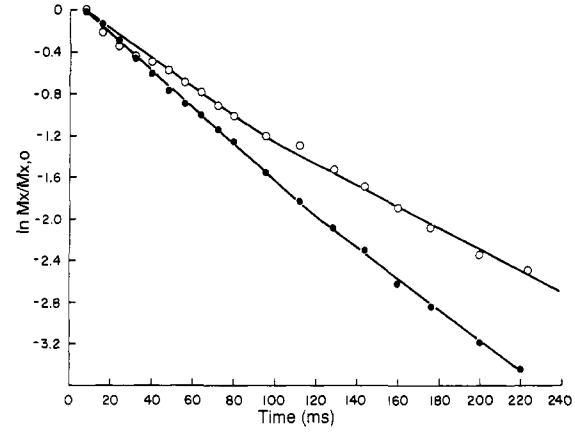

Figure 7. T_2 relaxation curves for DOC samples at concentrations of 15 mM (open circles) and 50 mM (closed circles) obtained with 4-ms delays between successive π pulses. Other parameters are the same as for Figure 5.

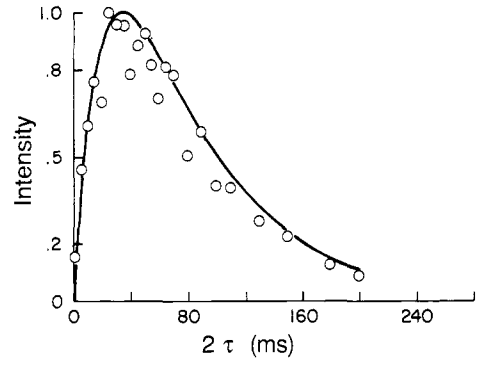

Figure 8. Forbidden peak intensity as a function of multiple quantum excitation time for methyl #18. Experimental points are indicated by the open circles, and the solid line is the best fit of the data. Parameters of the fit are indicated in Table III. A 50-mM DOC sample, 0.1 M Na_2CO_3, pD 9.0, was used.

the small departure from linearity, however, it is unlikely that an accurate determination of cross-correlation effects could be obtained through a fit of the T_1 and T_2 data alone.

The forbidden peak intensity profile displayed in Figure 8 provides additional evidence for cross-correlation effects. Their presence is more clearly demonstrated than in either T_1 or T_2 plots which show only slight departures from linearity. This clear demonstration is of great importance in cases where it is not possible to obtain a complete relaxation time course such as in a 2-D NMR analysis. In addition, forbidden peak intensity profiles obtained from one-dimensional NMR experiments complement T_1 and T_2 data sets. Hence, quantitation of cross-correlation spectral density terms seems more probable with observation of forbidden peak intensities than from exclusive use of either of the more standard T_1 or T_2 relaxation experiments. The line through the experimental points in Figure 8 is the best fit of the data obtained by simultaneously fitting T_1, T_2, and multiple quantum data sets.

While inclusion of both auto-correlation and cross-correlation dipolar spectral densities is required to produce this fit, the precise specification of random-field spectral densities is less critical. We have already mentioned that we are including random-field terms to describe relaxation of the A_3 spin system due to intra- and intermolecular dipolar interactions with external protons. In a molecular system as complex as DOC micelles there are no doubt a multitude of interactions, both inter- and intramolecular and all having potentially different correlation times, which contribute to the relaxation of the A_3 spin system. We have made no attempt to quantitate these interactions rigorously, and therefore we cannot a priori state what the absolute ratio of auto- and cross-correlation random-field terms is. We have attempted to determine how sensitive the fits of the data are to cross-correlation random-field

Table III. Parameters Obtained from NMR and Light Scattering Data

concn, mM	τ_0[a] (ns)	$\tau_\parallel$[b]	S	$j(0)$	$j(\omega)$
15[c]	2.64	5.33	1	0.761	6.41
15[d]	3.48	2.27	1	0.847	7.13
50[c]	4.62	2.17	1	0.751	9.71
50[d]	5.70	2.39	1	0.756	10.5
40[e]	4.44				

[a] Isotropic rotational correlation time. [b] Internal methyl rotation. [c] Fit obtained by setting auto- and cross-random-field terms equal. [d] Fit obtained by setting cross-random-field terms to zero. [e] Light scattering results.

terms and therefore how important it is to understand in a more quantitative way the processes which contribute to A_3 relaxation involving neighboring protons by considering two limiting cases. In the first case, we assume that cross-correlation random-field terms are negligible. This is a reasonable approximation in the limit where each of the three methyl protons is relaxed independently by external spins.[27] We have also fit the data by assuming equal contributions from both auto- and cross-random-field terms. Table III shows parameters obtained from the fits as well as micelle correlation times obtained from light-scattering measurements. We note that the parameters obtained by fitting the data are relatively insensitive to the inclusion of cross-correlation random-field terms and that the micellar size shows the same concentration dependence independent of whether such terms are included. This result suggests that while inclusion of random-field effects is required to obtain proper fits of the data, a detailed knowledge of the A_3 dipolar interactions with other protons is not required. Fits of T_1, T_2, and multiple quantum data are found to be inadequate, however, if auto-correlation random-field terms, $j(0)$ and $j(\omega)$, are not included. While the use of such terms to model inter- and intramolecular dipolar effects created by remote spins is clearly not rigorous for reasons outlined in the Theory section, a random-field approximation remains the most tractable approximation, and as the experimental data indicate, some contribution from this effect must be considered. Insensitivity to $j_c(0)$, the cross-correlation random-field term evaluated at $\omega = 0$, is considered further in the Appendix. We show that when slow motions dominate relaxation these terms do not contribute to forbidden peak intensities.

Some assessment of the reliability of other parameters in Table III can be obtained through theoretical simulations which systematically vary these parameters. Figure 9 shows theoretical forbidden peak intensity profiles as a function of overall micelle correlation time. The profiles were generated using the cone model, and the parameters used as indicated in the figure legend. The data were simulated using a computer program developed in this laboratory and discussed in a previous publication.[28] Of note is the fact that both the position of the maxima of these profiles and their intensities are exquisitely sensitive to the overall isotropic correlation time.

Finally, Figure 10 examines the sensitivity of the multiple quantum filtered relaxation experiment to the wobbling order parameter, S. While the amplitude, shape, and position of the maxima of the forbidden intensity profiles have similar dependencies on both τ_c and S, close inspection of Figures 9 and 10 shows that these dependences are not exactly the same, suggesting that both τ_c and S can be extracted from fits of the data. It also appears that the double quantum filtered relaxation experiment shows a greater sensitivity to S than T_2 relaxation profiles.

Discussion

Given the expected sensitivity of the experiments described here to overall correlation times and order parameters, one expects the data to give insight into the structure and dynamics of the micellar

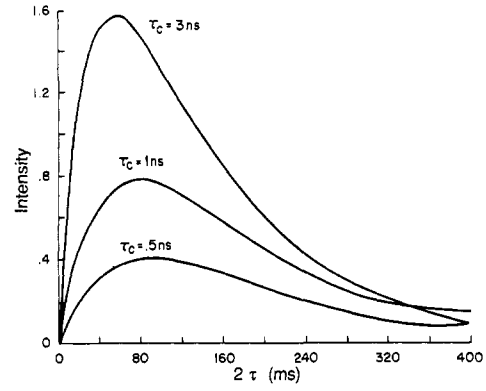

Figure 9. Theoretical forbidden peak intensity vs. excitation time for an A_3 spin system illustrating the sensitivity of this method to overall correlation time. Parameters used were $S = 1$, $\tau_\parallel = 5$ps, $j(\omega) = 0.5$, and $j(0) = 5.0$; auto- and cross-random-field terms were set equal.

system studied. As Table III indicates, the micelle rotational correlation times obtained from the NMR data show good agreement with the results from laser light scattering. In addition, excellent agreement is obtained with published ultracentrifugation data where a micelle correlation time of 3.6 ns at pH 9.0, 20 °C, and 0.3 mM NaCl was obtained.[29] Interpreting the micellar correlation times shown in Table III in terms of the Stokes–Einstein equation, and assuming the density of the micelle to be the same as that of the individual monomers, yields aggregation numbers of 25 and 40 for DOC at 15 mM, 0.1 M, Na_2CO_3, pH 9, and 50 mM, 0.1 M Na_2CO_3, pH 9, respectively. This is consistent with published literature values for DOC micelle aggregation numbers, 30, in 0.3 M NaCl at pH 9.[29] Of more interest is the fact that order parameters of unity are obtained for methyl #18 at concentrations of 15 and 50 mM DOC. A large order parameter might be expected since the methyl group is attached to a rigid steroid nucleus. Further, the result is consistent with current models of the DOC micelle which place the hydrophobic methyl groups in a rather well-structured interior.[19]

The experiments and results presented have implications which go well beyond the specific system studied. In 2-D NMR based structural analyses one of the outsanding problems involving the intrepretation of nuclear Overhauser effect cross-peak intensities, in terms of internuclear distance, stems from the fact that the NOE between a pair of spins is a function not only of their separation but also of the dynamics that govern their motion. While it is quite straightforward to separate contributions from dynamics and distance for the case of spins rigidly attached to a macromolecule, the interpretation of NOE cross-peaks associated with side-chain moieties having multiple degrees of freedom is not as simple. As an example consider the case of methyl groups in proteins. Often resonances from these groups are well-resolved in 2-D data sets and display well-defined NOE cross-peaks with neighboring residues. While these cross-peaks are potentially valuable for clarifying side-chain structure, they are frequently not used. Not only do the methyl groups have internal degrees of freedom which complicate their cross-relaxation behavior, but there is always the danger that the methyl groups in question may execute more complex motions which may have to be described in terms of order parameters less than one. If this is the case, then the distance obtained from an NOE cross-peak on the basis of a simple $1/r^6$ model would not be a meaningful reflection of the actual methyl group–neighboring proton distance. Extraction of methyl group order parameters using forbidden peak intensities would clarify whether NOE cross-peaks associated with a particular methyl could be used in a structure determination. Figure 10 suggests the feasibility of this approach since forbidden peak intensities in multiple quantum filtered data sets are shown to be highly sensitive to the cone order parameter, S. Moreover, the similarity of the pulse sequence used to generate our forbidden peak data to sequences used to acquire multiple quantum filtered

(27) Abragam, A. *Principles of Nuclear Magnetism*; Clarendon Press: Oxford, 1961.
(28) Kay, L. E.; Scarsdale, J. N.; Hare, D. R.; Prestegard, J. H. *J. Magn. Reson.* **1986**, *68*, 515.
(29) Small, D. M. *Adv. Chem. Ser.* **1968**, *No. 84*, 31.

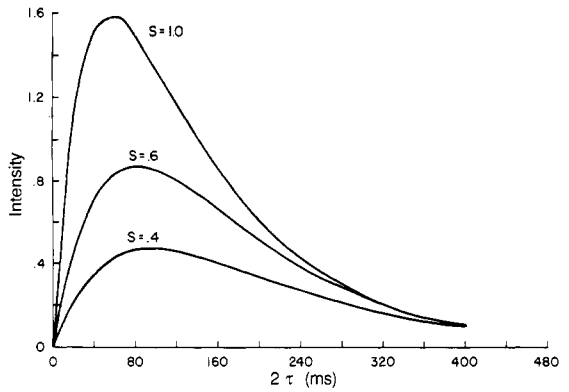

Figure 10. Theoretical peak intensity vs. excitation time for an A_3 spin system as a function of order parameter S. Parameters used were τ_c = 3 ns, $\tau_{||}$ = 5 ps, $j(\omega)$ = 0.5, and $j(0)$ = 5.0; auto- and cross-random-field terms were set equal.

COSY spectra suggests that some of the necessary data may be available in standard 2D data sets.

In addition, we wish to point out that extraction of cross-correlation spectral density terms may be of some assistance in separating inter- and intramolecular relaxation effects. Intragroup cross-correlation terms are much more effective than the former in producing forbidden peak intensity (see the Appendix). Such separations could prove important in understanding dynamics of molecular systems which are made up of several monomers such as in the case at hand.

In summary, we have demonstrated that forbidden peaks obtained in multiple quantum filtered spectra are useful for the extraction of dynamic information. The expected sensitivity to cross-correlation terms has been established, and the increased sensitivity to the cone order parameter S in comparison with conventional T_2 relaxation studies is an encouraging sign for the extension of this methodology to 2-D NMR data sets. Work is now in progress aimed at extending these initial results to the interpretation of forbidden cross-peak intensities from AX_3 spin systems in multiple quantum filtered 2-D data sets.

Acknowledgment. This work was supported by Grants GM-32243 and GM-33225 from the National Institutes of Health and by a predoctoral fellowship to L.E.K. from the National Sciences and Engineering Research Council of Canada. The research benefited from instrumentation provided through shared instrumentation programs of the National Institute of General Medical Science, GM 32243S1, and the Division of Resources of the National Institutes of Health RR02379.

Appendix

In this section we show, for an A_3 spin system in the limit of $\omega\tau_c \gg 1$, that nonzero dipolar cross-correlation terms are essential if elements of transverse magnetization, ρ_{14}, ρ_{47}, and ρ_{78}, are to relax differently. Differential relaxation of at least two of the three elements during the excitation time 2τ and during the acquisition time t in the pulse sequence depicted in Figure 2 is a necessary and sufficient condition for the generation of forbidden peaks in a double quantum filtered experiment.[3]

Since we consider the limiting case, $\omega\tau_c \gg 1$, we have neglected $J(\omega)$ and $J(2\omega)$ terms. While this is not fully justified for systems of moderate size, the results obtained show trends which approach a valid expression when molecules become large. From eq 4 and Table II we have that:

$$d\rho_{14}/dt = -3(J_A(0) + J_C(0))\rho_{14} \quad (A1)$$

$$d\rho_{26}/dt = (-J_A(0) + J_C(0))\rho_{26} + (-J_A(0) + J_C(0))\rho_{47} \quad (A2)$$

$$d\rho_{35}/dt = (-J_A(0) + J_C(0))\rho_{35} + (J_A(0) - J_C(0))\rho_{47} \quad (A3)$$

$$d\rho_{47}/dt = (-J_A(0) + J_C(0))\rho_{26} + (J_A(0) - J_C(0))\rho_{35} - 2(J_A(0) - J_C(0))\rho_{47} \quad (A4)$$

$$d\rho_{78}/dt = -3(J_A(0) + J_C(0))\rho_{78} \quad (A5)$$

Equations A1 and A5 can be integrated immediately to yield

$$\rho_{14}(t) = \rho_{14}(0)\exp(-3(J_A(0) + J_C(0))t)$$
$$\rho_{78}(t) = \rho_{78}(0)\exp(-3(J_A(0) + J_C(0))t) \quad (A6)$$

Equations A1, A2, and A4 can be rearranged to give

$$\frac{d}{dt}\begin{bmatrix}\rho_{26}\\ \rho_{35}\\ \rho_{47}\end{bmatrix} = (J_A(0) - J_C(0))\begin{bmatrix}-1 & 0 & -1\\ 0 & -1 & 1\\ -1 & 1 & -2\end{bmatrix}\begin{bmatrix}\rho_{26}\\ \rho_{35}\\ \rho_{47}\end{bmatrix} \quad (A7)$$

which can be solved using eq 9 to yield:

$$\rho_{47}(t) = \tfrac{1}{3}(\rho_{26}(0) - \rho_{35}(0) + 2\rho_{47}(0))\exp(-3(J_A(0) - J_C(0))t) \quad (A8)$$

Equations A6 and A8 show that in general ρ_{47} will decay differently from either ρ_{14} and ρ_{78}. However, in the absence of cross-correlation spectral density terms, i.e., $J_C(0) = 0$, all three transverse elements decay with the same time constant. Hence, no magnetization would be detected in a multiple quantum filtered experiment without finite $J_C(0)$.

The effects of the random field term in eq 3 on elements of transverse magnetization, ρ_{14}, ρ_{47}, ρ_{78}, can also be easily understood in the limit of $\omega\tau'_c \gg 1$, where τ'_c is the effective correlation time describing random-field interactions. In the treatment that follows, we neglect the contributions to relaxation due to intragroup dipolar effects. Since the random-field Hamiltonian does not couple with the dipolar Hamiltonian, separation of contributions is rigorously correct. From Table II we obtain:

$$d\rho_{14}/dt = -j_a(0)\rho_{14} \quad (A9)$$

$$d\rho_{78}/dt = -j_a(0)\rho_{78} \quad (A10)$$

$$\frac{d}{dt}\begin{bmatrix}\rho_{26}\\ \rho_{35}\\ \rho_{47}\end{bmatrix} = (j_a(0) - j_c(0))\mathbf{0}\begin{bmatrix}\rho_{26}\\ \rho_{35}\\ \rho_{47}\end{bmatrix} \quad (A11)$$

with

$$\mathbf{0} = \begin{bmatrix}-1 & {}^1/_3 & {}^2/_3\\ {}^1/_3 & -1 & {}^{-2}/_3\\ {}^2/_3 & {}^{-2}/_3 & {}^{-2}/_3\end{bmatrix} - j_a(0)\mathbf{1} \quad (A12)$$

where $j_a(0)$ and $j_c(0)$ are auto- and cross-random-field terms, respectively, evaluated at $\omega = 0$, and $\mathbf{1}$ is the identity matrix. These equations are readily solved to give:

$$\rho_{14}(t) = \sqrt{3}\exp(-j_a(0)t) \qquad \rho_{78}(t) = \sqrt{3}\exp(-j_a(0)t)$$
$$\rho_{47}(t) = 2\exp(-j_a(0)t) \quad (A13)$$

where $(\sqrt{3}, 1, -1, 2, \sqrt{3})$ have been substituted for $(\rho_{14}(0), \rho_{26}(0), \rho_{35}(0), \rho_{47}(0), \rho_{78}(0))$.

A comparison of eq A6 with eq A13 shows that the decay of transverse elements ρ_{14}, ρ_{47}, ρ_{78} is more sensitive to intragroup (A_3) dipolar effects than random-field effects, as expected. In addition, eq A13 shows that random fields, unlike dipolar fields, create a uniform decay of transverse elements regardless of the magnitude of $j_c(0)$. This implies, at least for the limiting case $\omega\tau'_c \gg 1$ considered here, that nonzero random-field cross-terms are not sufficient for the excitation of multiple quantum coherence in an A_3 spin system.